

## 6. Problem •8: Electrostatics

### *Solution of Croatia*

#### Problem •8: Electrostatics

Josko Jelacic<sup>1</sup>, Marin Lukas<sup>1</sup>, Milan Markovi•<sup>2</sup>, Damjan Pelc<sup>1</sup>, Ivan Sudic<sup>1</sup>

<sup>1</sup> V. Gimnazija, Klaićeva 1, 10000 Zagreb, Croatia

<sup>2</sup> XV. Gimnazija, Jordanovac 8, 10000 Zagreb, Croatia

#### **The Problem:**

*Propose and make a device for measuring the charge density on a plastic ruler after it has been rubbed with a cloth.*

#### **Abstract**

We present a computer numerically controlled surface charge density analyzer for measuring mono-layer surface charges in medium resolution on dielectric surfaces. The device is based on a solid state FET electrometer coupled with an optically referenced electrostatic mill enabling accurate phase-locked measurements. The scanning and control are obtained with a two-dimensional computer controlled discrete step translator capable of delivering up to 20 steps per second. The device was demonstrated in a measurement of the surface charge density on a plastic ruler rubbed with a cotton cloth.

#### **1. Introduction.**

The problem of non - contact charge measurement on different dielectrics is of greatest interest nowadays. From microscopic applications to atmospheric electricity recording, charge detectors of various designs are implemented. In this article we will discuss the construction of such a device, intended for measurements in the medium resolution range (that is, neither atomic – scale nor large charge structures like atmospheric electricity), intended for measuring the charge density of a flat charge monolayer on a dielectric surface. We will demonstrate its action in a measurement of the charge accumulated on a plastic ruler rubbed with a cloth, a system being very favorable for testing the device resolution and precision due to large charge gradients on a small surface area. But before we proceed to the description of the device, we must note some general characteristics our charge detector should have; in the end we will see how many requirements we have fulfilled. First of all, the spatial resolution for the suggested application should be at least a few millimeters due to the large gradients, and better if possible. The charge measurement resolution isn't as critical; the charges normally accumulating on a ruler can be quite large, as we shall see. Anyway, a higher charge resolution means a more reliable device. The third important parameter is the time the measurement takes. We will find that charge continuously drifts away from our ruler; this is unavoidable except by putting the entire device in an inert atmosphere or vacuum, which was too complicated for us to do. Although the drifting can be minimized by several techniques (to be discussed), a fast measurement is necessary. As our device will in fact be a scanner, moving across the ruler surface and measuring local charge density, we must be careful to minimize the number of needed scanning steps to shorten the measurement time, while

retaining an acceptable spatial resolution. We will discuss these matters in more detail when we get to the actual device construction.

## 2. The Ruler.

As we have mentioned, our charge analyzer will be used on a charged plastic ruler. Our ruler was made of polymethylmetacrilate and was 15 cm long and 3 centimeters wide. The charging of a ruler by rubbing it with a cloth is a high school demonstration in electrostatics, and there is a number of charge *detection* (not measurement!) methods suiting it. The most common are different electrometers based on charge – metal needle repulsion, and charged powders (like sulphur) clinging to the charged regions of the ruler. However, really *measuring* the charge density distribution with a reasonable spatial resolution is a considerable difficulty. Even more complicated is the process of charging; why are electrons transferred between cloth and ruler surface, and what sign will the net charge on the ruler have? The answer to these questions has to do with intermolecular forces on surfaces, delocalized electrons in the fabric and on the plastic, dielectric polarization and so forth, and we will not go into tackling with it. Even the sign of the charges is not uniquely determined; we have measured both positive and negative charges on one and the same ruler, which was quite a surprise. The important fact is that once the charges are deposited on the ruler surface they basically *do not* move. This is due to the fact that the ruler is a dielectric, meaning that it has a huge electrical resistance and no current can flow either inside it or on its surface. Another important consequence of this is that the charges will always stay on the surface and never penetrate the material; thus we can rightly speak of a monolayer. However, in practice the conductivity of the ruler surface usually isn't nearly as small as one would expect, mainly because of the grease and dirt deposited on the ruler when it is handled. This can cause significant charge drift and make measurements rather inexact. To minimize this effect the ruler needs to be degreased thoroughly (we rinsed it in ethyl alcohol several times before every measurement) and put on nonconducting stands (in our case degreased ceramic cylinders). In this way the charge drift can be slowed down considerably, though it can never be completely removed – there is namely a second source of drift, humidity in the atmosphere. Due to the polar nature of the water molecules in air the charges on the surface may cling to them and escape the ruler. This drift is very difficult to remove; in all of our experiments the air was constantly held dry (humidity under 20%), but a certain drift was always present. However, the charge didn't change as rapidly as to influence the measured results significantly, as we managed to get the scanning time down to a few minutes.

The rubbing process itself was devoted special care. With a clean cotton cloth the ruler was rubbed exquisitely at one or two localized spots, the rest remaining more or less untouched. In this way we created regions of large charge density and steep transitions to low – charge regions; this enabled us to test the capabilities of our detector. A good device should be capable of reconstructing such configurations in detail.

## 3. The Device.

### 3.1. Principle of measurement.

The number of charge measurement principles and devices developed to date is enormous, and each has its advantages and drawbacks. Some of the most common are the Kelvin and vibrating capacitor probes [1] (for medium spatial resolution), cantilever – based systems [2] (used in atomic force microscopes, measure the force on a charged tip with atomic – scale spatial resolution), the already mentioned crude electrometers used in demonstrations, solid

state electrometers [3] of various designs, and many more. Our device used a combination of a so-called *electrostatic mill* and a solid state electrometer. The electrostatic mill is a movable grounded plate, periodically covering and uncovering the electrometer's detector lead. In this way the electrometer is only exposed to the field it measures for short periods of time, yielding an alternating signal. If the phase relationship between the mill oscillations and the periodic electrometer signal is established, one can perform phase – locked measurements to eliminate virtually all noise. Thus the field can be measured to a very high precision. However, there is another vital element in the construction of our device, namely the scanning system. The mill, electrometer test lead and phase reference measuring system were all mounted on a compact probe, which had to be moved across the ruler surface in order to scan the charge density distribution. This was done with a custom made xy-translator, controlled electronically. In the following sections we will describe these parts one by one, in order to gain insight in the construction and operation of our apparatus.

### 3.2. The Probe.

The probe, being the core of the system, requires special attention. As we have mentioned, its main parts are the electrostatic mill, electrometer test lead and phase reference measuring system. All those elements were mounted on a large grounded metal plate which provided shielding and a homogeneous field in the perpendicular direction (Fig. 1.). The mill, as the only moving part, required precision; it consisted of a conducting thin disc (made of paper covered with a conducting graphite film) with three holes cut in it, attached to a small DC motor (similar to the ones used in mobile phones for vibration). The mill (or "chopper", as we refer to it) is shown in Fig. 2. It rotated with a frequency of about 80 Hz, providing a convenient modulation of the electrometer signal. The electrometer itself was based on a FET (short for field effect transistor), which is a semiconductor device consisting of a long slab of n – doped material (through which a current is set to flow) and two smaller sheets of p – doped material located on opposite sides of the n – slab. If leads are connected to those sheets and put in an electric field, charges in the sheets are dislocated, effectively altering the volume (and thus the resistance) of the n – doped slab (Fig. 3.). This means that one can determine the strength of the field by measuring the current flowing through the n – slab! It is clear that the resistance between the points A and B in figure 3 is enormous (ideally infinite), meaning that charges aren't lost from the test leads but respond only to the outside field. However, the problems arising to instabilities and noise when using a sole FE transistor made us choose the FET amplifier LMC 6062 instead. The principle of operation remains practically the same. The amplifier was connected to be noninverting, with a gain equal to unity and with a low – pass RC filter at the input to serve as a first, crude noise removal facility. The entire circuit was closed in a grounded metal box shielding it from outside influences (Fig. 4.), while the test lead consisted of a copper disc 1 mm in diameter, mounted in a fitting hole in the probe grounded plate. The third vital part of the probe was the phase reference. It had to feed an appreciable signal to the used lock – in amplifier in order for it to be capable of comparing phases. We used a simple photodiode (the bright spot in Fig. 2.); the signal from it was smaller when it was covered by the dark chopper and larger when a hole was under it. The frequency of the signal was of course equal to the chopper frequency. However, the signal offset (due to the constant light always falling on the diode) had to be removed, and the alternating signal amplified. This was done with a LM741 opamp with adjustable gain, followed by a passive high – pass filter for removing the offset. The amplifier and its circuit were enclosed in a grounded box as well.

Once having the two signals, measurement and reference, we fed them into a lock – in amplifier in order to remove noise. As the phase relationship between the measurement signal and the reference was always constant, a phase – locked loop could do a good job removing all out-of-phase or wrong frequency noise, and the resulting signal was very clean and stable. With such noise removal we were capable of measuring the voltage from the FET amplifier with nanovolt precision. As we will see, this amounts to a charge measurement sensitivity of about 10 or even 1 nC/m<sup>2</sup>, while the typical charge densities on the ruler are of the order of 10 μC/m<sup>2</sup>.

### 3.3. Scanning and Control.

Having constructed the probe, we were left with the task of building a device which would move it across the ruler surface in order to obtain a charge density map. The general requirements for such a system we have mentioned already: high spatial resolution and speed. Another problem is the synchronization with the measuring system; this we solved by putting one single computer in charge of both. The translator itself was built from the remains of two used printers (one printer for the  $x$  and one for the  $y$  direction) and driven by two unipolar stepping motors. Driving the motors in accordance, with directions given by the main computer was entitled to a microcontroller mainboard. The mainboard was a complicated circuit containing two 8051 microcontrollers clocked at 12 MHz, communicating with the computer via a serial link. Communication proceeded both ways, enabling precise scanning control: the computer collects a number of signal voltage values from the lock-in (using a 12 bit AD converter) and forms their average (that is another low – pass filter!), and then orders the mainboard to move the probe to the next measuring position. When the mainboard reports that the probe has moved a new set of voltages is collected, and so on. The schematic of the entire apparatus is given on Fig. 5, and a photograph on Fig. 6. The spatial resolution was set to 1 mm, and the device was capable of delivering up to 20 measurements per second. However, to use it we had to perform calibration.

### 3.4. Calibration.

To be able to measure the charge in absolute units (like C/m<sup>2</sup>) we had to calibrate our device in a known field. This was done as follows. An aluminum disc, having a surface much larger than the test lead, was held at a constant, known potential  $V$ . The probe was put above it, at a height  $D$ . The probe grounded plate thus created a *charge image* of the disc, the system being equivalent to a capacitor at voltage  $V$  and plates  $D$  centimeters apart. Due to the fact that both the probe plate and the charged disc were much larger than the test lead (or the distance  $D$ , for that matter), the field at the test lead location was almost homogeneous, with a vertical component

$$E_z = \frac{V}{D} \quad (1)$$

Now the root-mean-square voltage measured from the detector,  $U_{RMS}$ , we found to be proportional to  $E$  over a large voltage range (Fig. 7.), following the relationship

$$E_z = 1.88 \cdot 10^6 U_{RMS} \quad (2)$$

We were able to distinguish between positive and negative charges thanks to the phase-locked measurement method; the photodiode always gives the same signal, but the phase of the measurement signal is reversed when measuring different signs of charge. This means that the sign of the measured signal will correspond to the sign of the charge. It is also very important to note that only the  $z$  – component of an electric field can influence the test lead due to the

grounded plate; it creates a mirror image of the charges measured, thus virtually eliminating lateral components. Also, the test lead is a thin disc, so lateral charge displacement in it shouldn't have a significant effect on the FET.

Having performed the calibration, we were ready to make field scans of the ruler and calculate the real charges from the measured field. This was also a troublesome task, due to the fact that the distance between probe and ruler was always kept at 5 mm; this is a large distance compared to the sensing lead disc, which means that a relatively large charged area influences the signal. To maximise the spatial resolution in charge determination we will have to solve a system of equations for the charges; we will return to that issue in due time.

#### 4. Measurement and Charge Calculation

Before conducting charge maps measurements, we had to check how fast the charge was leaking off the ruler and how this could influence our scans. Two static measurements were performed, one with the ruler uncleaned and one with a degreased ruler (Fig. 8.). The probe wasn't moving during one measurement. The results are striking: the dirty ruler loses charge at a large pace (70% in five minutes), while upon degreasing it the loss is brought down to about 10% during five minutes! As the scan time was about three minutes, the losses during scanning could be neglected. However, if a necessity for high precision is shown one can always compensate for the loss using the curve on Fig. 8.

Measuring the charges on the ruler was conducted for two rubbings; the first measurement had 5796 and the second 4991 one-millimeter steps. As we mentioned already, the distance between detector and ruler was held at a constant 5 mm. The obtained field maps are shown on Fig. 9. After determining the field maps, we had to calculate the real charge. This charge is easy to find if we divide our ruler into little rectangles, each having a net charge  $\sigma_i$ ; let the sides of the rectangles have lengths equal to the step size, and let their number be equal to the number of steps  $N$ . The field one such rectangle causes at the probe location is simply

$$\mathbf{E}_i(\mathbf{r}_s) = \frac{1}{4\pi\epsilon_0} \frac{\sigma_i \Delta x \Delta y}{|\mathbf{r}_s - \mathbf{r}_i|^2} \hat{\mathbf{r}} \quad (3)$$

where  $\mathbf{r}_s$  is the probe radius-vector,  $\epsilon_0$  is the permittivity of the vacuum,  $\Delta x$  and  $\Delta y$  the side lengths of the rectangle (in our case both equal to the step size),  $\mathbf{r}_i$  the radius-vector of the rectangle and  $\hat{\mathbf{r}}$  a unit vector lying on the line which connects the rectangle and the probe (it can also be written as  $\frac{\mathbf{r}_s - \mathbf{r}_i}{|\mathbf{r}_s - \mathbf{r}_i|}$ ).

Summing the fields of all rectangles and multiplying by two (the charge images forming on the grounded plate double the field!) one gets the net field at the probe location; the detector is only influenced by the vertical component:

$$E_z(x_s, y_s) = \frac{h}{2\pi\epsilon_0} \sum_{i=1}^N \frac{\sigma_i \Delta x \Delta y}{\left[ (x_s - x_i)^2 + (y_s - y_i)^2 + h^2 \right]^{\frac{3}{2}}} \quad (4)$$

where  $x_s$  and  $y_s$  are the probe coordinates,  $h$  its distance from the ruler,  $N$  the number of rectangles (and steps) and  $x_i$  and  $y_i$  the rectangles' coordinates. The probe makes  $N$  steps in its measurement, and on each location measures the field (4). In this way we obtain a system of

$N$  equations for exactly  $N$  unknown charge densities! Of course, the scanning region has to be as large as the ruler so that the  $N$  rectangles cover the entire charged surface. The system of equations is linear, with an extended matrix of the form

$$\begin{pmatrix} \xi_{11} & \xi_{12} & \cdots & \xi_{1N} & E_{z1} \\ \xi_{21} & \xi_{22} & \cdots & \xi_{2N} & E_{z2} \\ \vdots & \vdots & \ddots & \vdots & \vdots \\ \xi_{N1} & \xi_{N2} & \cdots & \xi_{NN} & E_{zN} \end{pmatrix} \quad (5)$$

with the coefficients  $\xi$  equal to

$$\xi_{si} = \frac{h}{2\pi\epsilon_0} \frac{\sigma_i \Delta x \Delta y}{\left[ (x_s - x_i)^2 + (y_s - y_i)^2 + h^2 \right]^{3/2}} \quad (6)$$

As the number  $N$  in our measurements was around 5000 (the system matrix thus containing tens of millions of coefficients), we had to solve the system (5) with the help of a computer. A program diagonalizing the system matrix and solving the resulting triangular form for the unknowns  $\sigma_i$  (Gauss algorithm) was written in Turbo Pascal. The results were charge density maps (Fig. 10.), with spatial resolution 1 mm. As we see, the charge on the ruler was typically of the order of  $10 \mu\text{C}/\text{m}^2$ , as we mentioned before; this is quite a large charge density, corresponding to a metal plate at potentials as high as several thousand volts. The surprising fact is that one can obtain both signs of charge in a single rubbing; the maps clearly show this. We suspect that the reasons for this are very complicated and have to do with intricate surface effects; a possible explanation would be the repelling of charges on the ruler: if a large negative charge is put on the surface it may repel other dislocated electrons. They move away from the negative charge, leaving bare protons behind which form a positive patch. This is however not quite plausible because of the huge resistance to electron flowing; a very high field indeed would be required. A better explanation would probably have to do with the rubbing and transport process itself, but the complications are enormous, so we won't tackle with it. Our task of *measuring* the charge density is complete, with rather satisfactory results.

## 5. Conclusion.

To conclude we will shortly sum up the properties of our device. The charge scanner we constructed was based on a solid state FET electrometer modulated with a chopper; the charge density distribution on a charged ruler (or similar dielectric surface) can be measured fast and reliable. The spatial resolution is 1 mm (this can be made even better, but the scanning time grows proportionally), the sensitivity is about  $10 \text{ nC}/\text{m}^2$  (it can also be enhanced by using more accurate electronics) and a scan of about 5000 points takes three minutes; the measured charge loss during this time is about 5%. We can see that we have more or less fulfilled all the desired characteristics mentioned in the Introduction. In the end let us propose an application we think is quite amusing: charge writing. If one has a relatively large dielectric plate, writing on it with charges is possible with a high voltage tip; if the voltage is high enough a discharge through air will deposit electrons on the plate on a small region near the tip. Putting the tip on

a xy translator enables one to write or make pictures (Fig. 11.). The writing can easily be read with our detector. Of course, a similar process is already implemented in printers and photocopying machines: the xerox process!

We thank our mentors dr. sc. Željko Marohnić from the Institute of Physics for advice, discussions and providing the instruments used in measurement, and prof. Dario Mičić for support and help with everything.

#### References.

- [1] A. Winter, J. Kindersberger, Measurement of Double Layer Surface Charge Density Distribution on Insulating Plates with Capacitive Probes, Int. Conference on Advances in Processing, Testing and Application of Dielectric Materials, Wroclaw, 2001., paper 31.
- [2] W. F. Heinz, J. H. Hoh, Relative Surface Charge Density Mapping with the Atomic Force Microscope, Biophys. J. 1999., vol. 76, no. 1.
- [3] W. Mauderli, F. P. Bruno, Solid State Electrometer Amplifier, Phys. Med. Biol., 1966., vol. 11.

#### Figures:

Fig. 1. – The probe

Fig. 2. – The chopper.

Fig. 3. – The principle of operation of a FE transistor electrometer

Fig. 4. – The FET amplifier circuit in a grounded box

Fig. 5. – The schematic of the entire apparatus.

Fig. 6. – The entire apparatus

Fig. 7. – The calibration curve.

Fig. 8. – The measurements of charge in time. The detector was static for both curves.

Fig. 9. The field scans. The colour scale is in arbitrary units (volts from the detector)

Fig. 10. – The charge maps.

Fig. 11. – Charge drawing

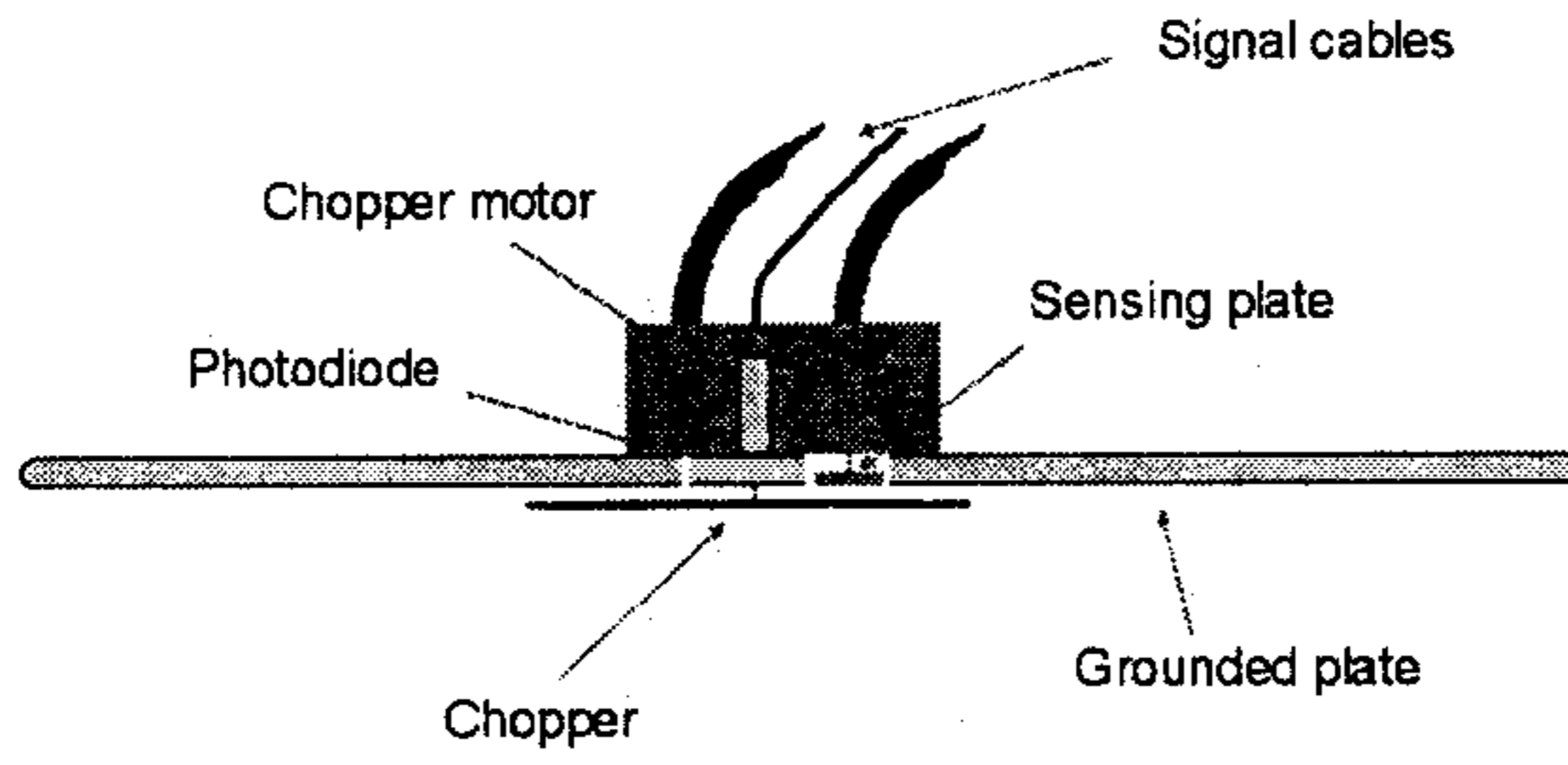


Fig.1

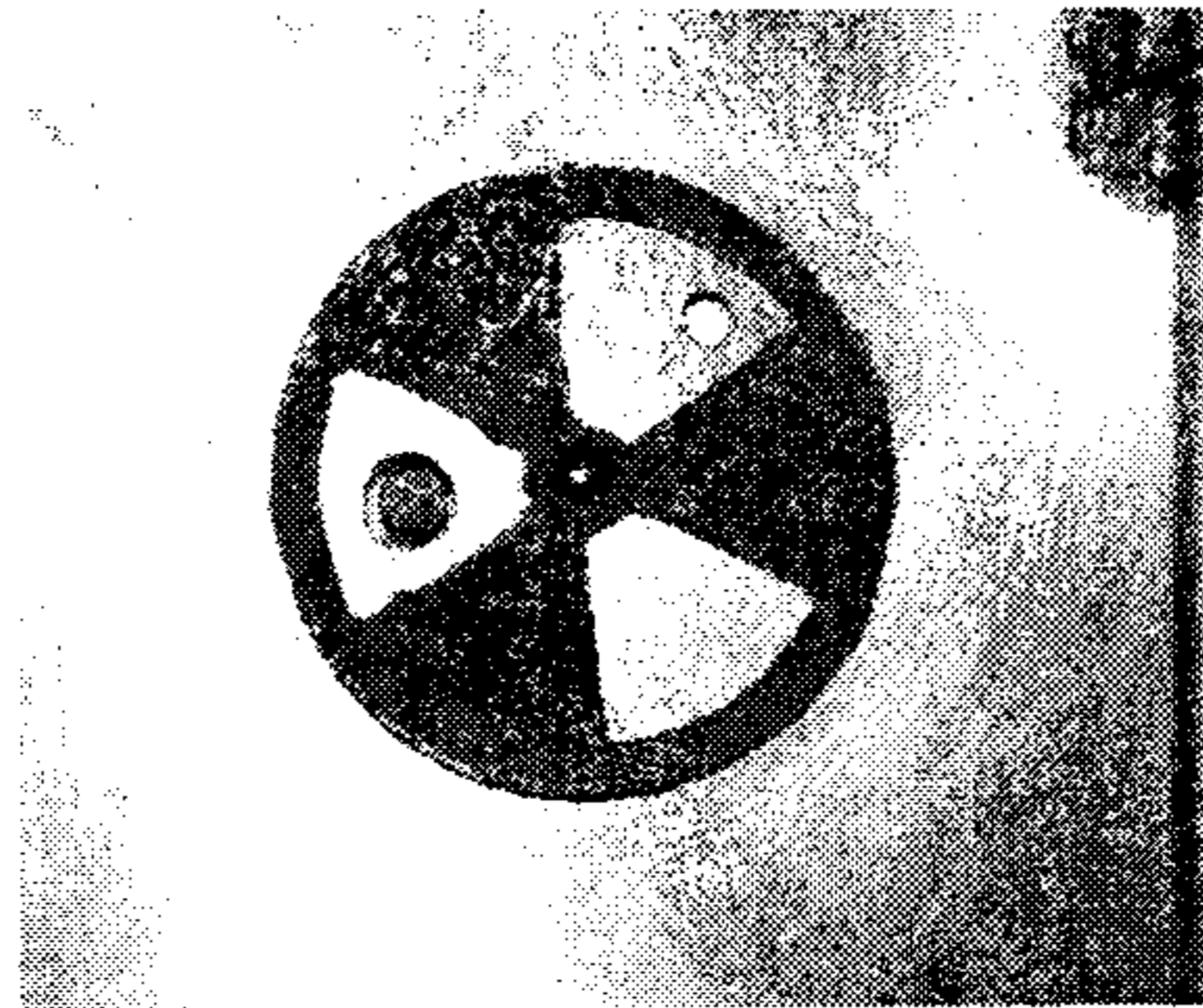


Fig.2

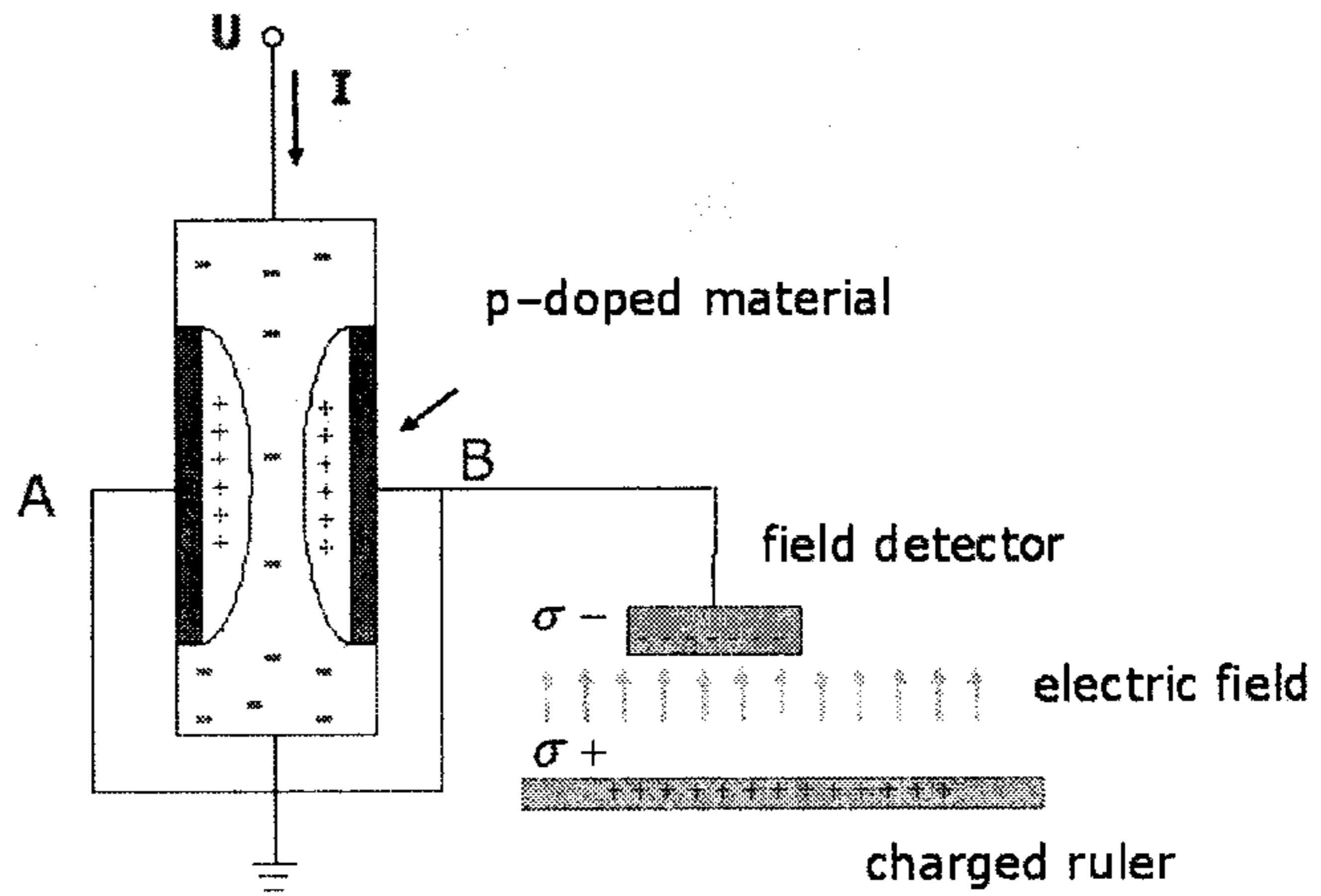


Fig.3



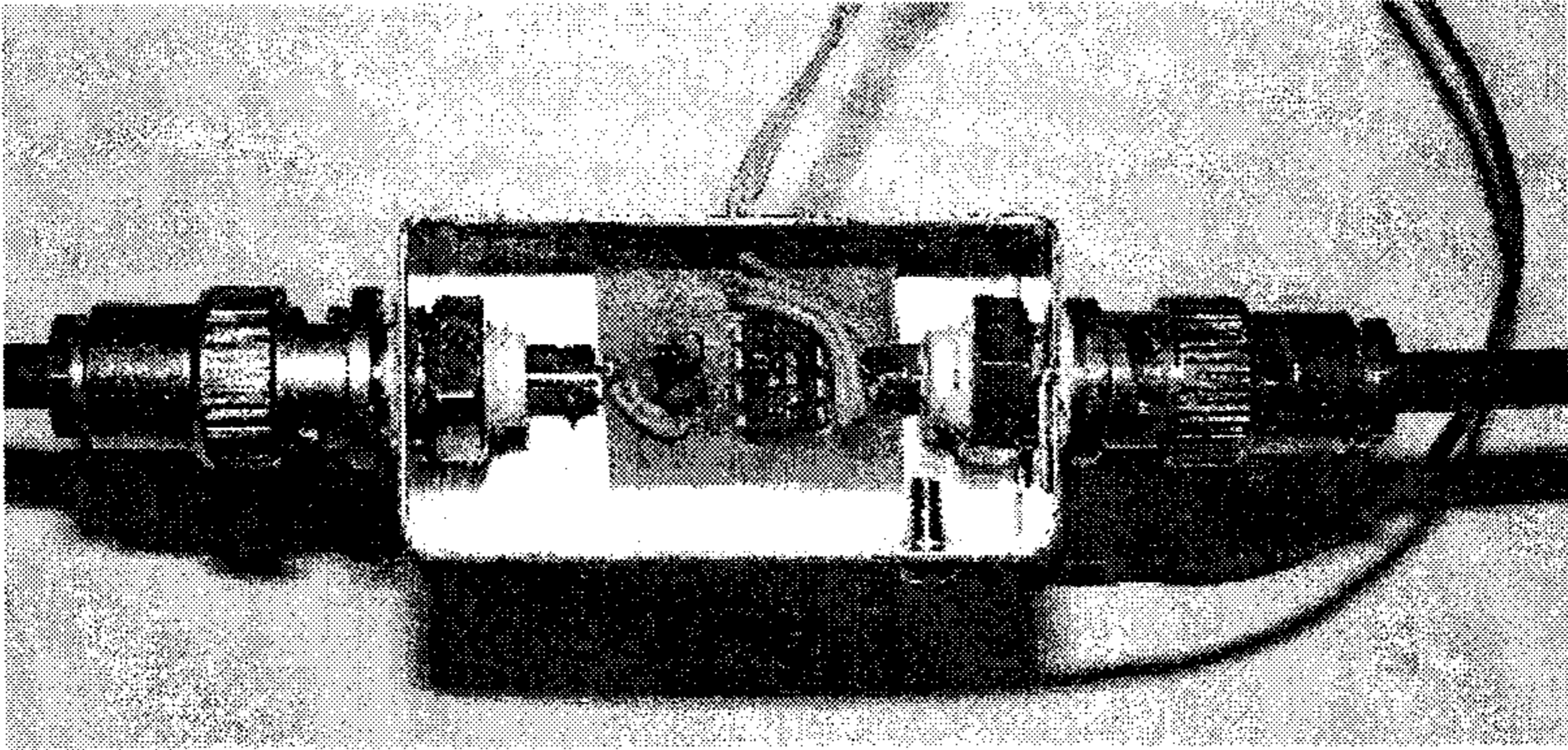


Fig.4

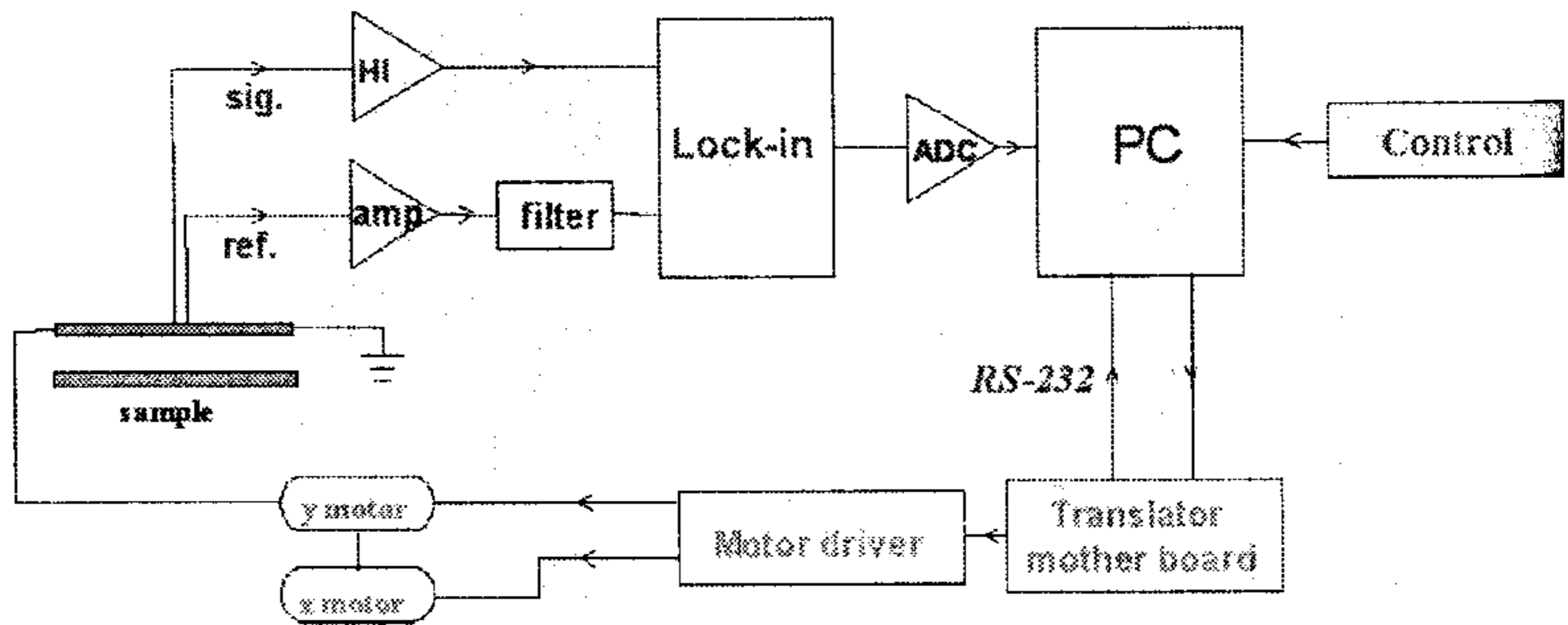


Fig.5



Fig. 6

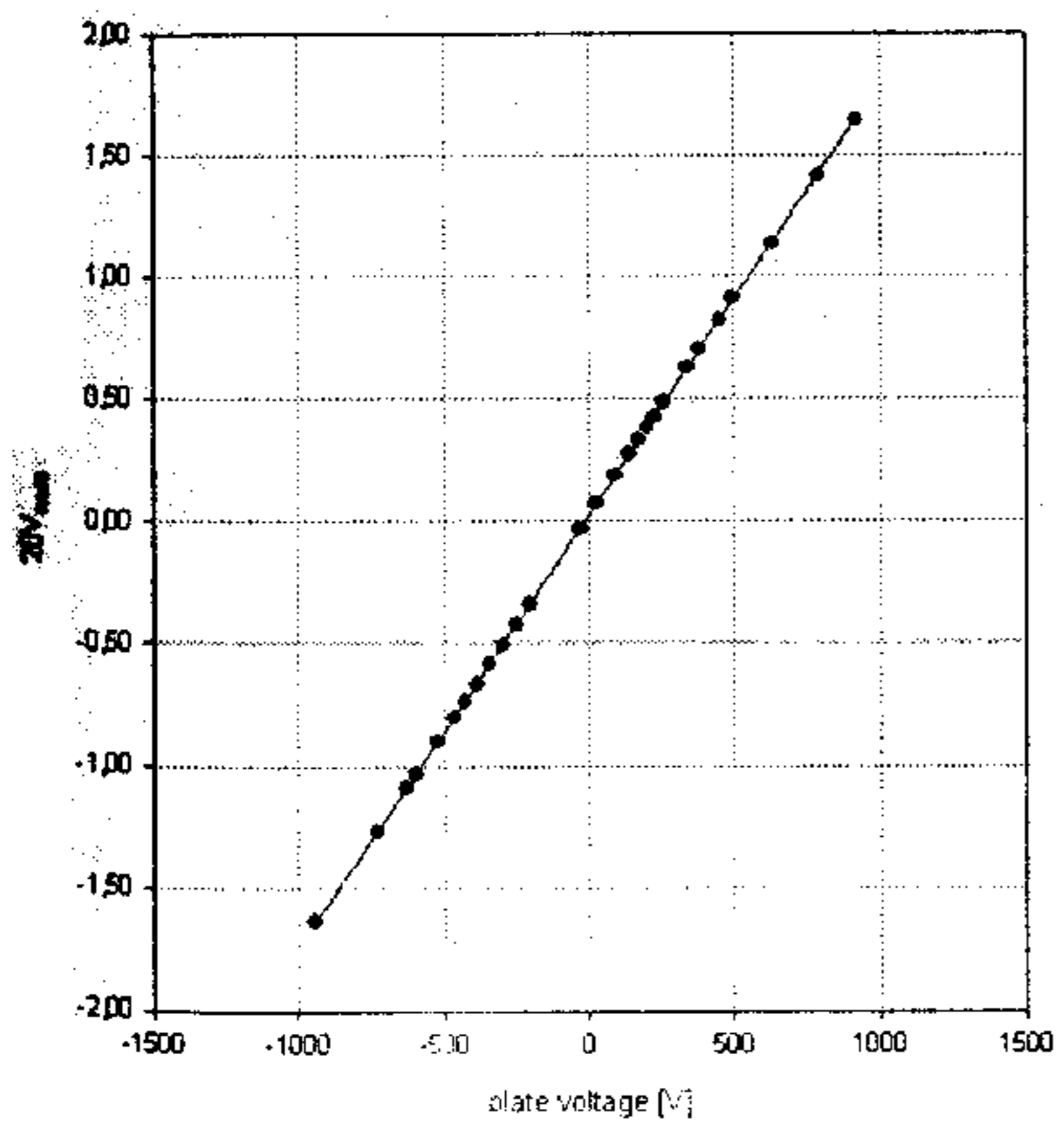


Fig. 7

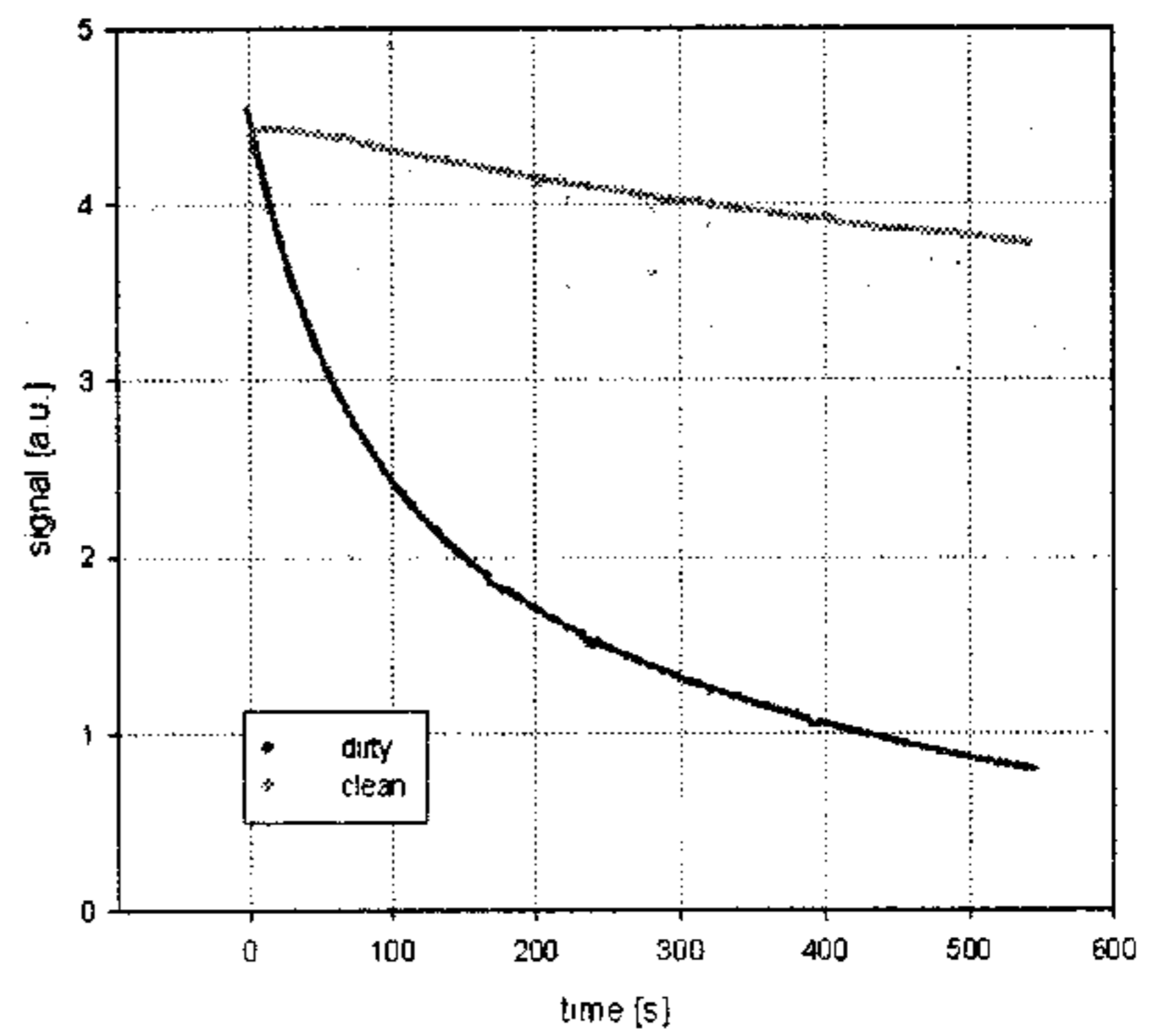


Fig. 8

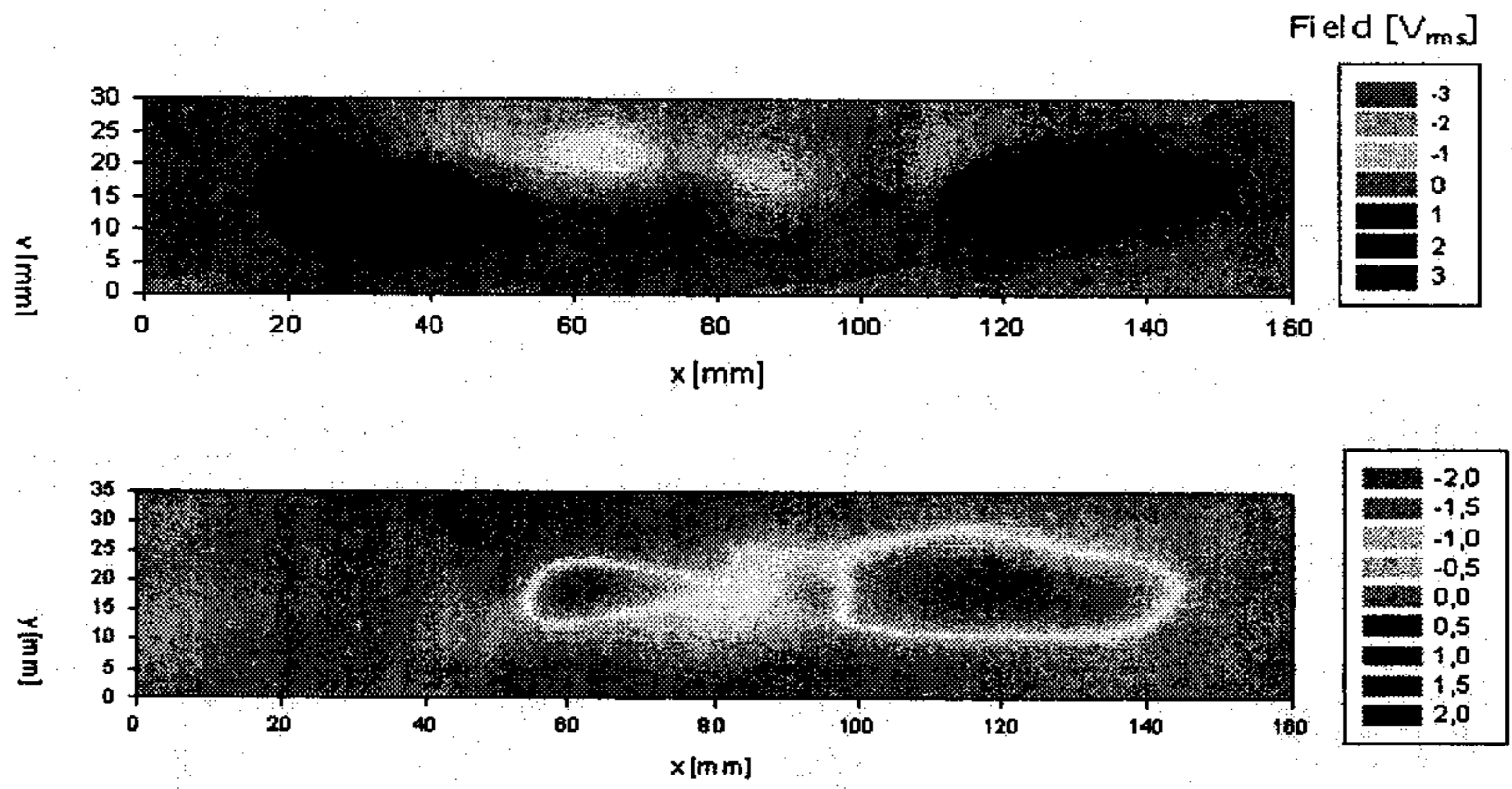


Fig.9

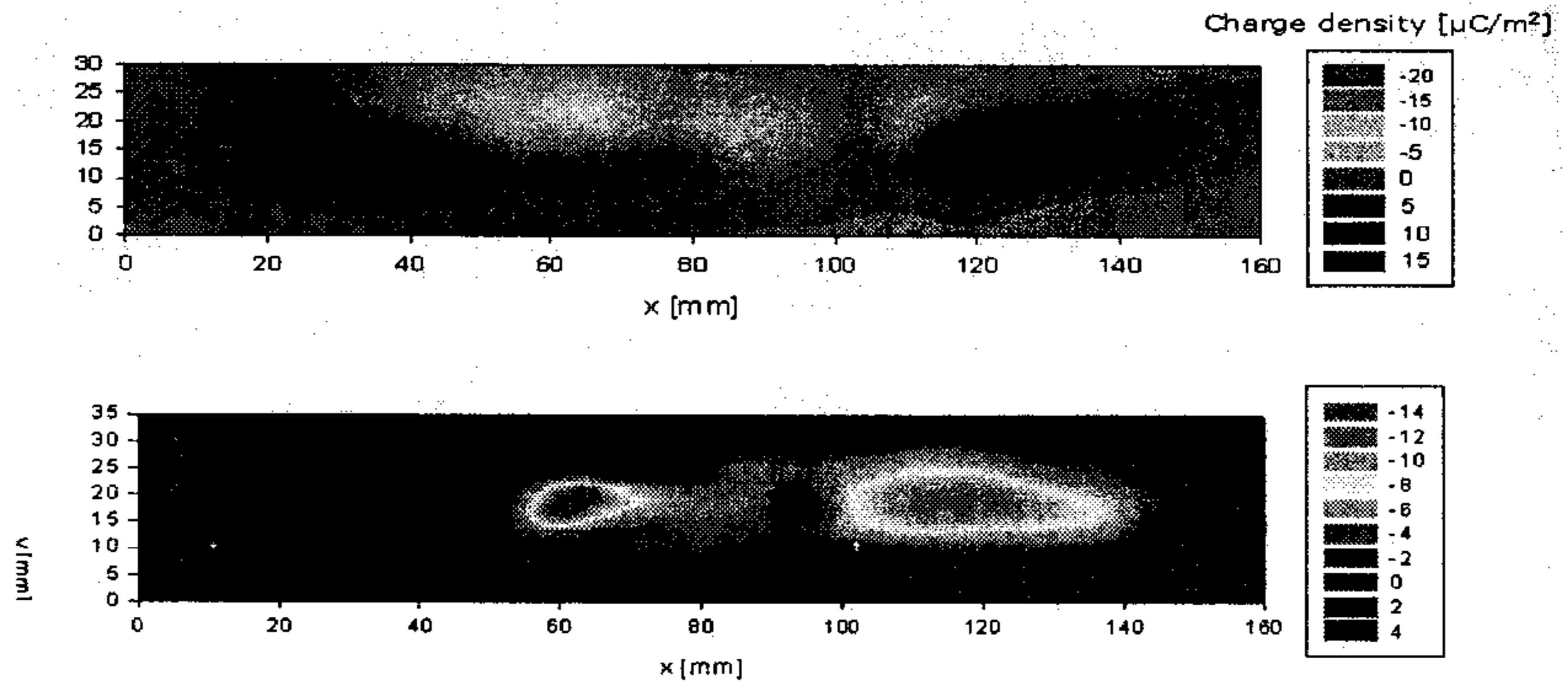


Fig.10

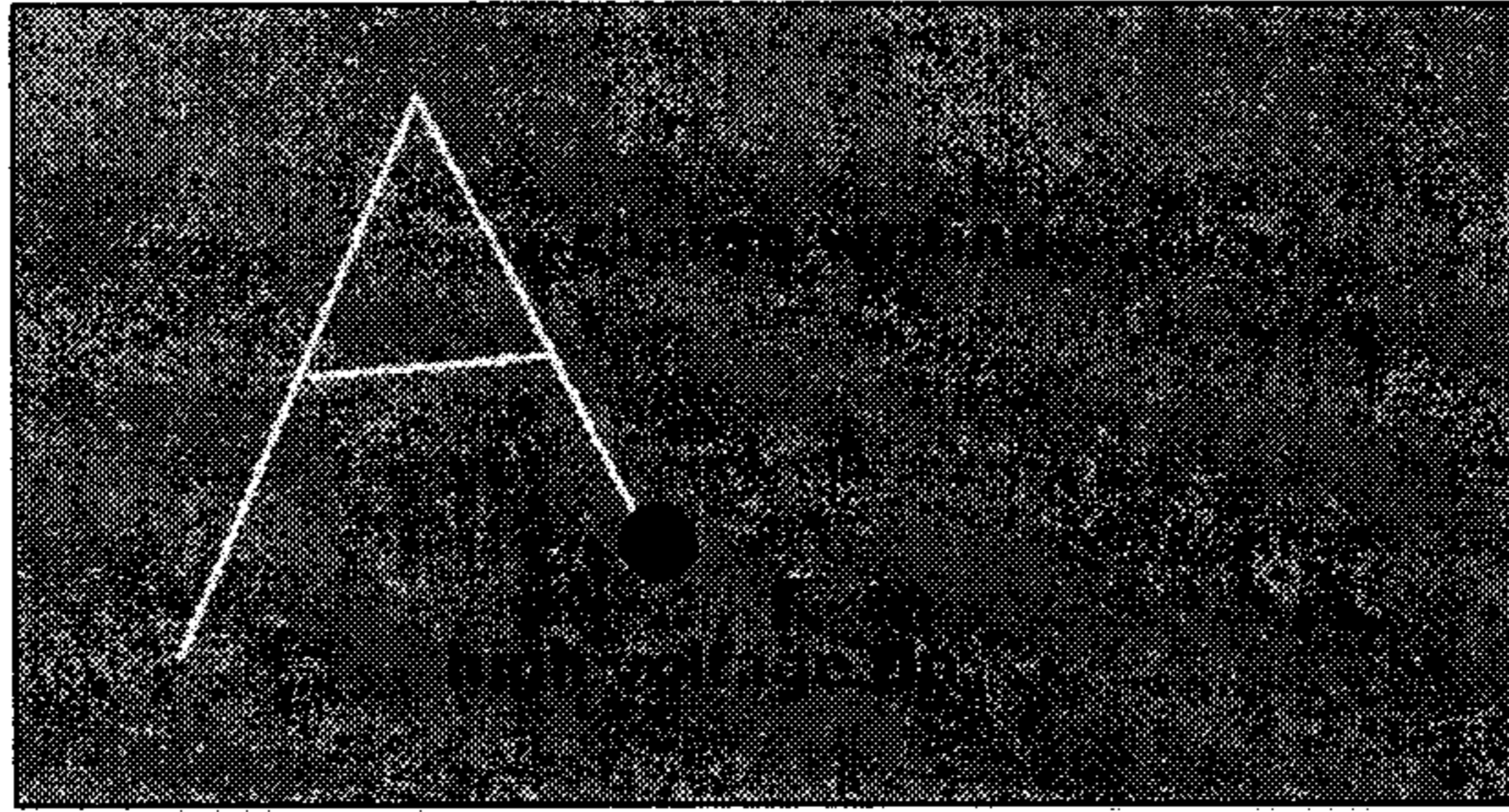


Fig.11

## 7. Problem №10: Inverted pendulum

### 7.1. Solution of Korea

#### Problem №10: Inverted pendulum

Park, Hyeongsu, Korean Minjok Leadership Academy  
1334 Sosa Anheung Hoengsung Gangwon, Korea 225-823

#### The Problem:

*It is possible to stabilize an inverted pendulum It is even possible to stabilize an inverted multiple pendulum /one pendulum the top of the other/. Demonstrate the stabilization and determine on which parameters this depends.*

This paper studies comprehensively about the methods of stabilizing an inverted pendulum. An inverted pendulum is a free hung pendulum which is upright, and just like an ordinary pendulum, it naturally falls downward because of gravity. Thus, the inverted pendulum system is inherently unstable. In order to keep it upright, or stabilize the system, one needs to manipulate it, either vertically or horizontally.

Many stabilizing methods have been developed. In 2-Dimensional system, an inverted pendulum can be stabilized thorough either vertical or horizontal oscillation with certain frequency. In 3-Dimension, rotational arms or free robot arms are used for stabilization. For algorithm, a controller using feedback system or simple oscillation both work to keep the pendulum upright, though processes or extents of stability are different from each other.

This paper first proposes theoretical background for all the cases. Then, the experiments focus on horizontal oscillation and delve into the various characteristics and factors of stabilization pattern.